THE JOURNAL OF BIOLOGICAL CHEMISTRY VOL. 290, NO. 16, pp. 10071–10082, April 17, 2015

Obstructor A Organizes Matrix Assembly at the Apical Cell Surface to Promote Enzymatic Cuticle Maturation in *Drosophila*[*]

Received for publication, September 26, 2015, and in revised form, March 2, 2015 Published, JBC Papers in Press, March 3, 2015, DOI 10.1074/jbc.M114.614933

Yanina-Yasmin Pesch[‡§1], **Dietmar Riedel**[¶1], **and Matthias Behr**[‡§2]

From the [‡]*Department of Molecular Developmental Biology, Life & Medical Sciences Institute (LIMES), University of Bonn, 53115 Bonn, Germany, the* [§]*Department of Cell & Developmental Biology, Translational Centre for Regenerative Medicine (TRM), University of Leipzig, 04103 Leipzig, Germany, and the* [¶]*Electron Microscopy Group, Max-Planck-Institute for Biophysical Chemistry, 37077 Göttingen, Germany*

Background: The apical extracellular matrix (aECM) protects against environmental stresses that attack organisms throughout lifetime.
Results: Epidermal cells secrete obstructor A into a core organizer region for controlling aECM assembly at the apical cell surface.
Conclusion: Normal aECM assembly is mediated by obstructor A and regulates cuticle stability at the epidermis.
Significance: Cuticle formation of the insect epidermis is genetically conserved.

Assembly and maturation of the apical extracellular matrix (aECM) is crucial for protecting organisms, but underlying molecular mechanisms remain poorly understood. Epidermal cells secrete proteins and enzymes that assemble at the apical cell surface to provide epithelial integrity and stability during developmental growth and upon tissue damage. We analyzed molecular mechanisms of aECM assembly and identified the conserved chitin-binding protein Obst-A (Obstructor A) as an essential regulator. We show in *Drosophila* that Obst-A is required to coordinate protein and chitin matrix packaging at the apical cell surface during development. Secreted by epidermal cells, the Obst-A protein is specifically enriched in the apical assembly zone where matrix components are packaged into their highly ordered architecture. In *obst-A* null mutant larvae, the assembly zone is strongly diminished, resulting in severe disturbance of matrix scaffold organization and impaired aECM integrity. Furthermore, enzymes that support aECM stability are mislocalized. As a biological consequence, cuticle architecture, integrity, and function are disturbed in *obst-A* mutants, finally resulting in immediate lethality upon wounding. Our studies identify a new core organizing center, the assembly zone that controls aECM assembly at the apical cell surface. We propose a genetically conserved molecular mechanism by which Obst-A forms a matrix scaffold to coordinate trafficking and localization of proteins and enzymes in the newly deposited aECM. This mechanism is essential for maturation and stabilization of the aECM in a growing and remodeling epithelial tissue as an outermost barrier.

A critical feature for organisms is the formation and integrity of the outermost barrier to protect their body against dehydration, invading pathogens and toxic environments. Epidermal, gut, and tracheal cells deposit apical extracellular matrix (aECM)[3] components at the apical surface where they need to assemble. The insect aECM provides an exoskeletal cuticle that is in contact with the surrounding environment for protection against lethal infections and other environmental stresses. The developmental progress of larvae requires repetitive molting (ecdysis), the replacement of old by new cuticles, to accommodate increasing body size. Therefore mechanisms that coordinate assembly and maturation of all new cuticles are critical for barrier integrity. Even though production and degradation are well described in insects (1–6), the regulatory processes of forming compact aECM barriers remain poorly understood.

Chitin synthases are active at the apical cell membrane where they produce nascent chitin polymers (1–3). Deposited at the apical cell surface, chitin polymers spontaneously form microfibrils of varying length and diameter (3). A systematic assembly of the chitin-based aECM generates a prominent and stable part of the growing exoskeletal cuticle (7). Therefore, during late larval stages, existing compact cuticles need to stretch when new matrix is deposited at the apical cell surface for increasing overall cuticle thickness and stability. Additional enzymatic modifications, such as deacetylation, promote essential cuticle maturation of the aECM (8–11). Chitin deacetylation fundamentally improves chemical and physical matrix properties of organs, tissues, and even engineered materials (12, 13). However, mechanisms that control the aECM formation during larval molting, and at larval intermolt, when the cuticles receive their compact organization but need to be flexibly stretched (14), are yet unknown.

Obst-A is a member of the *obstructor* multigene family, which is highly conserved among arthropods and expressed in

* This work was supported by Deutsche Forschungsgemeinschaft Grant SFB645-C5 (to M. B.).
[1] These authors contributed equally to this work.
[2] To whom correspondence should be addressed. Tel.: 49-341-97-39584; Fax: 49-341-97-39589; E-mail: matthias.behr@uni-leipzig.de.

[3] The abbreviations used are: aECM, apical extracellular matrix; Cbp, chitin-binding probe; WGA, wheat germ agglutinin; qRT-PCR, quantitative real time PCR; Obst-A, Obstructor-A; Knk, Knickkopf; Serp, Serpentine; Verm, Vermiform.

chitin-producing epithelia (15). Homologous *obstructor* genes were recently also identified in beetles (CPAP3 (cuticular proteins analogous to peritrophins 3)), mosquitos, and other insects (16–18). In *Drosophila*, the Obst-A chitin-binding protein interacts with the deacetylation domain protein Serp (Serpentine) and the chitin protector Knk (Knickkopf) to prevent premature degradation of the tracheal matrix in late embryos (19). Here we define a new Obst-A-dependent chitin matrix organizing center in the epidermis, the yet uncharacterized assembly zone, which links the epidermal epithelium with the formation of a highly organized cuticle exoskeleton. The role of the assembly zone is to modulate aECM assembly at the cell surface for protecting animals during molting and upon wounding.

EXPERIMENTAL PROCEDURES

Fly Stocks and Genetics—Flies were derived as described below: white^{1118} (w-; here referred to as wild type), *btl*GAL4, 69BGal4 driver lines and *knk*^{f0192} (Bloomington stock center), *mega*^{VE} (20), *obst-A*^{d03} (19), *serp-verm* double mutant (10), UAS-RNAi-*serp*, UAS-RNAi-*verm* and UAS-RNAi-*knk* fly lines were obtained from the Vienna stock center. To distinguish mutants from others, balancer chromosomes were used: FM7i,P{ActinGFP} or TM3,P{GAL4*twi*.G}2,3P {UAS-2xEGFP} or TM3*ser*P{w[+m]*hsp70*:GAL4}P{w[+m]UAS:GFP}. The absence of GFP expression was used as a marker to identify larvae carrying hemizygous and homozygous mutant alleles. Transheterozygous mutants were generated by mating of *obst-A*/FM7i,P {ActinGFP} heterozygous females with either *serp,verm*/TM3,P {GAL4*twi*.G} 2,3P {UAS-2xEGFP} or knk/TM3*ser*P{w[+m]*hsp70*:GAL4}P{w[+m]UAS:GFP} heterozygous males. The non-GFP offspring of first instar larvae, collected and tested for cuticle integrity, include 50% of *obst-A* hemizygous and 50% of transheterozygous mutants. Because of early larval lethality of *obst-A* hemizygous null mutants, analyzed non-GFP offspring collection for immunofluorescent stainings at second and third instar larvae only contained transheterozygous mutants. Crosses of 69BGal4 driver flies and UAS-RNAi-*knk*, *-serp*, and *-verm* flies, respectively, result in RNAi-mediated knockdown in the offspring epidermis.

Antibodies and Microscopy—Larvae were fixed overnight in 4% paraformaldehyde at 4 °C, dehydrated, and embedded in JB-4 Plus (Polysciences, Warrington, PA). Polymerized blocks were cut in 7-μm sections (Ultracut E; Reichert-Jung, Solms, Germany). Sections were rehydrated and subjected to an antigen retrieval protocol in 10 mM sodium citrate, pH 6.0, at 65 °C depending on the primary antibody for 15 min (α-Obst-A and α-Knk) or 1 h (α-Serp, α-Verm) and incubated with 0.001% trypsin in 0.05 M Tris-HCl, pH 8.0, at 37 °C for 1 h. Sections were blocked in PBS + 10% donkey serum for 30 min and stained overnight at 4 °C with Alexa 488-conjugated chitin-binding probe (Cbp; 1:100; New England Biolabs, Ipswich, MA), which selectively binds chitin. The Alexa 633-conjugated wheat germ agglutinin (WGA; 1:250; Molecular Probes, Carlsbad, CA) is a lectin, which is able to react with internal sugar residues of glycoproteins and selectively recognizes *N*-acetylneuraminic acid and *N*-acetylglucosamine. WGA has a very strong affinity to chitin and was used to label the apical cell surfaces in *Drosophila* embryos and larvae (19, 21–23). Embryo fixation and antibody stainings were performed as described previously (19, 21, 22).

The antibodies used are α-Spectrin (1:10, mouse, Developmental Studies Hybridoma Bank), Knk (1:333; rabbit) (24), Obst-A (1:300; rabbit) (19), Serp (1:175; rabbit), and Verm (1:175; rabbit) (10). Primary antibodies were detected by secondary antibodies linked with fluorescent dyes (Dianova, Hamburg, Germany and Jackson ImmunoResearch Laboratories, West Grove, PA) and mounted in Vectashield (Vector Laboratories, Burlingame, CA). For Z-stack analysis sequential scans were taken with Zeiss LSM710/LSM780 microscopes (Carl Zeiss) and a 63× LCI Plan Neofluar objective. The pinhole was adjusted to "airy unit 1," and standard settings were used. Images were cropped in ImageJ and Adobe Photoshop CS6, and figures were designed with Adobe Illustrator CS6.

Ultrastructure Analysis—Larvae were placed on a 150-μm flat embedding specimen holder (Engineering Office Wohlwend, Sennwald, Switzerland) and frozen in a Leica HBM 100 high pressure freezer (Leica Microsystems, Wetzlar, Germany). An automatic freeze substitution unit (Leica) was used for embedding of the vitrified samples. Substitution was performed at −90 °C in a solution containing anhydrous acetone, 0.1% tannic acid, and 0.5% glutaraldehyde for 72 h and in anhydrous acetone, 2% OsO_4, 0.5% glutaraldehyde for additional 8 h. After 18 h of incubation at −20 °C, warmed (4 °C) samples were washed with anhydrous acetone and embedded in Agar 100 (Epon 812 equivalent). Images were taken with a Philips CM120 electron microscope (Philips Inc.; TemCam 224A slow scan CCD camera; TVIPS, Gauting, Germany). Indirect detection of chitin was carried out on Epon-embedded samples as previously described by Moussian *et al.* (25) using immunogold labeling of WGA recognizing chitin. WGA labels colloidal gold, an electron dense marker used to study chitin localization in ultrastructure analysis (26). WGA (5 μg/ml; Vector Laboratories) was detected by a rabbit-anti-biotin antibody (3.9 μg/ml; Rockland, Gibbertsville, PA) and protein A gold (10 nm, 1:100, G. Posthuma, Utrecht, The Netherlands). As negative control immunogold labeling without WGA was performed, as well as without primary antibody. These negative controls showed no significant unspecific labeling (data not shown).

We performed Obst-A immunogold labeling on ultrathin sections of HM20-embedded samples as follows. The high pressure frozen larvae were substituted using the Leica automatic freeze substitution unit for 57 h at −90 °C in 1% uranyl acetate in acetone. After further incubations at −60 and −25 °C, the samples were infiltrated with HM20 resin (Polysciences) and polymerized using UV light at −45 °C for 48 h. Immunogold labeling of Obst-A was performed using 1:100 diluted Obst-A antibody and protein A gold (10 nm, 1:50). For better visibility of the gold labeling, pictures were taken of not counterstained sections using a Philips CM120 electron microscope (Philips Inc.; TemCam F416 CMOS camera; TVIPS).

Cuticle Integrity Test, Survival Assay, and Body Size—Cuticle integrity was tested with a thin glass needle. Mid-first instar larvae were laterally pricked at the posterior part, and hemolymph bleeding was monitored. Organ spill out after injury was considered as a defect in cuticle integrity. For the survival assay,

100 stage 17 embryos of each genotype were placed alive on apple juice agar plates with yeast (25 embryos/plate). The number of surviving animals was counted throughout larval and pupal development until the hatching of adult flies. To determine overall body size, body circumference in cross-sections of first instar wild type and *obst-A* mutant larvae was measured (in pixels) with ImageJ. The average radius of the sections was determined (in pixels) for calculation of the ideal circumference ($2\pi r$). The actual circumference was compared with the ideal circumference, and the discrepancy was statistically analyzed. Calculations were performed for 5 larvae/genotype. For all experiments, significance was calculated using a *t* test (Microsoft Excel), and *p* values are represented by *asterisks*: *, $p < 0.05$; **, $p < 0.01$; and ***, $p < 0.001$. The *error bars* show S.E. for the integrity test and standard error for the survival assay.

Quantitative Real Time PCR—obst-A mutant first instar larvae and wild type larvae from different developmental time points were grown at 25 °C, collected, and homogenized in a Precellys homogenizator. RNA was extracted using the NucleoSpin RNA II kit (Macherey-Nagel, Düren, Germany), and cDNA was synthesized using the QuantiTect kit (Qiagen). Quantitative real time PCR (qRT-PCR) was performed with a CFX96 cycler (Bio-Rad). For normalization, transcript levels of *rp49* (ribosomal protein L32) were used. qRT-PCRs were carried out of at least five individual biological replicates. Standard control PCRs (no template control; negative control) were used to rule out contaminations. In addition, primer efficiency (above 95%), as well as potential dimer formation, was evaluated. As a control *obst-A* null mutant larvae did not show *obst-A* expression (data not shown), which is consistent with previous findings (19). Significance was tested using one-way analysis of variance (GraphPad Prism 6), and *p* values are indicated by asterisks (*, $p < 0.05$; **, $p < 0.01$; and ***, $p < 0.001$). The *error bars* show the S.E. The following primers were used for qRT-PCR analysis: *obst-A*-for, GCAGTGCGACAAGTTCTACG; *obst-A*-rev, GAACTTGCGGTTGAG-TGGAT; *serp*-for, CAAGGCCACCTACTTCGTGT; *serp*-rev, ACTGCGATCTCGTGTCCTTT; *verm*-for, GTGGCTGAAGTCGAAGAAGG; *verm*-rev, TTGGTCACGAAGAACACGTC; *knk*-for, GGGGCGGATACGTTTTTCTG; *knk*-rev, TCCAGAATGTTGGTTTTGCCAT; *ribosomal protein L32* (rp49)-for, GCTAAGCTGTCGCACAAATG; and rp49-rev, GTTCGATCCGTAACCGATGT.

RESULTS

The chitin matrix is the main part of the cuticle that is essential for epidermal stability. Barrier integrity is required for survival and shaping of organisms and organs throughout development. Therefore, a number of scaffold proteins and enzymes coordinate chitin matrix assembly, maturation, and degradation at the apical surface of epidermal cells. The Obst-A chitin-binding protein is fundamental for the barrier function of embryonic and larval exoskeletal cuticles. Severe molting defects and lethality at transition to second instar stage in null mutant larvae suggested that Obst-A plays an essential role in cuticle matrix formation (19).

It has been demonstrated that endogenous Obst-A binds chitin (19). Obst-A protein sequence analysis predicted three subsequent type 2 chitin-binding domains (15). The stereotypic pattern of the three Obst-A chitin-binding domains suggested a function in chitin assembly in epithelial organs that require tight and strong cuticles (15). We investigated whether Obst-A is involved in modulating the epidermal chitin matrix structure. This was addressed by analyzing the overall shape and the ultrastructure of late first instar larval cuticle. The wild type chitin matrix, specifically marked by the Cbp, was evenly formed at the epidermal apical cell surface. Cross-sections revealed in 97% of late first instar wild type larvae ($n = 27$) that epidermis and attached cuticle straightly lined a rounded body (Fig. 1*A*). In contrast, 54% of late first instar *obst-A* mutant larvae ($n = 24$) showed an extremely wrinkled and massively deformed body shape in cross-sections (Fig. 1*A*). This phenotype is new and unique among known chitin regulators. In addition, nearly one-third (29%) of the larvae revealed cuticle detachment from epidermal cells (Fig. 1*B*), whereas wild type was normal. To study body shape, the relationship between wrinkled cuticle appearance and body size was investigated in wild type and *obst-A* mutants (each $n = 5$). We measured the actual circumference of first instar cross-sections and the average radius for calculating the ideal circumference. In wild type larvae, the actual cuticle circumference was increased by 9% compared with the ideal circumference because of only a few protrusions and notches. In *obst-A* mutant larvae, the size of the buckling cuticle was significantly increased (*, $p < 0.05$), with a discrepancy with the ideal circumference of 48%. These findings show that normal body appearance depends on Obst-A function during larval development.

The well defined epidermal cuticle morphology can be visualized in ultrastructure analysis and comprises the outermost envelope, the epicuticle, and the inner chitin-rich procuticle. During larval growth, the procuticle develops a highly organized architecture of condensed chitin fibrils which form an increasing number of regularly stratified chitin lamellae observed in second instar larvae (Fig. 2*A*). Importantly, the epidermis contains a distinct and less electron condensed layer between the apical cell surface and the chitin-rich procuticle (Fig. 2*A*). This defined layer has been previously described as the assembly zone (27), which is synonymous to adhesion zone (28) and the deposition zone (14). In the process of cuticle formation, the assembly zone is a stable and permeable matrix, passed by newly synthesized chitin components, but its function in cuticle formation is not yet understood (14, 27, 28). In contrast to the wild type, the less electron condensed assembly zone was not detectable in *obst-A* mutant larvae. Instead, the procuticle-like structure filled the entire region between epicuticle and epidermal cell surface (Fig. 2*A*). To further distinguish the procuticle from the assembly zone, we performed immunogold labeling using WGA, which possesses a strong affinity to oligomers and polymers of *N*-acetylglucosamine (26). In ultrastructure studies of wild type larvae, WGA-gold conjugates were enriched in the compact chitin-rich procuticle, but not within the assembly zone (Fig. 2, *B* and *C*). In *obst-A* mutants, WGA appeared evenly distributed throughout the entire chitin matrix (Fig. 2, *B* and *C*). Our findings show that a normal assem-

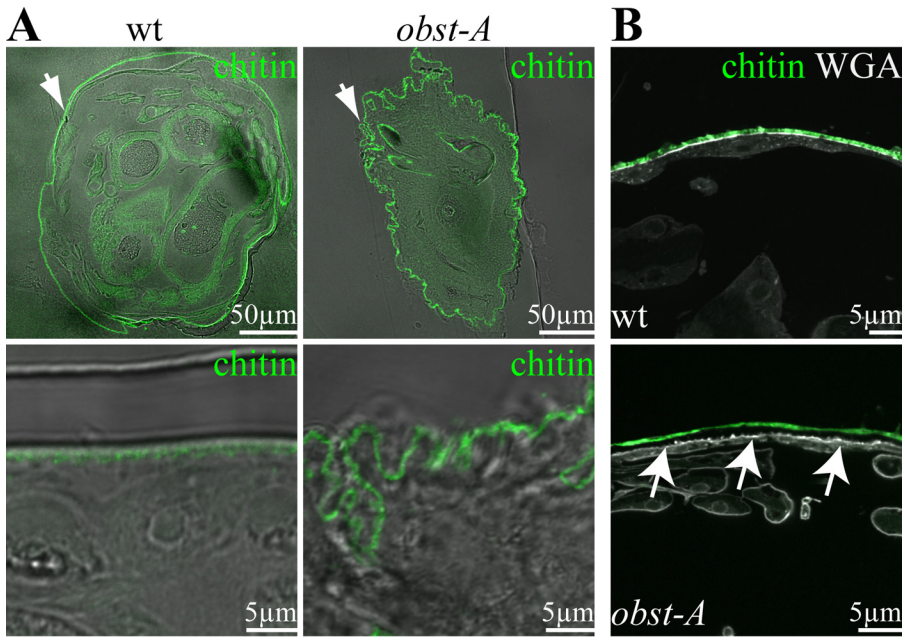

FIGURE 1. **Obst-A is required for larval body shape control and epidermal cuticle integrity.** *A* and *B*, confocal and bright field (*bf*) images show larval cross-sections. Chitin is visualized by Cbp (*green*) and WGA (*gray*, *B*) marks on the apical cell surfaces. *A*, in 97% ($n = 27$) of wild type first instar larvae the cuticle (*green*) is evenly attached to the epidermal cells. In 54% ($n = 24$) of *obst-A* mutant first instar larvae, the epidermal cuticle is wrinkled, and the body circumference is increased. Images are generated by confocal sections and bright field microscopy. The *upper panels* show cross-sections of the larvae (*arrows* point to the epidermis), and the *lower panels* show magnifications of the epidermal cuticle. *B*, in 97% ($n = 27$) of wild type larvae, the cuticle is tightly attached to epidermal cells and marked by WGA. In 29% ($n = 24$) of *obst-A* mutant larvae, the cuticle was detached (*arrows*) from the underlying epidermal cells (*arrows*). *Scale bars* represent 50 or 5 μm, respectively.

bly zone between apical cell surface and procuticle was strongly reduced or even absent in *obst-A* mutant epidermis.

We next considered whether Obst-A is involved in epidermal chitin matrix assembly. In wild type second instar larvae, ultrastructure analysis revealed that the chitin matrix becomes highly organized into multiple chitin layers (Fig. 2*A*). In contrast, normal chitin assembly was impaired in *obst-A* mutants, resulting in a defective procuticle (Fig. 2*A*). Chitin matrix defects would further explain the detached cuticle and wrinkled body shape caused by the loss of cuticle robustness in *obst-A* mutants (Figs. 1, *A* and *B*, and 2*A*). These observations provide evidence that Obst-A is involved in epidermal cuticle formation.

Given that Obst-A is required in the epidermal cuticle assembly zone, we examined its expression by epidermal cells. We performed immunofluorescent labeling studies in the embryonic and larval epidermis by using an antibody that specifically recognizes Obst-A (19). In late wild type embryos, epidermal Obst-A protein was apically enriched at the extracellular surface, and only little intracellular staining was detected (Fig. 3*A*), suggesting that Obst-A is secreted by the epidermal cells. This is consistent with the findings that late embryos start to secrete cuticle components before larval hatching (14). For a number of matrix proteins, apical deposition depends on septate junction function (11). The claudin-like Mega (Megatrachea) is a core component of septate junctions forming at the lateral membrane in many epithelia including the epidermis (20). Disrupting septate junctions in *mega* mutant embryos led to intracellular enrichment and extracellular reduction of Obst-A in epidermal cells (Fig. 3*B*). The *Drosophila* deacetylases, Serp and Verm, are required for late embryonic epidermal cuticle formation. In contrast to *mega*, *serp,verm* double mutant embryos showed normal secretion of epidermal Obst-A toward the developing cuticle (Fig. 3*C*).

Cuticle secretion is continued during the early first instar larval stage. Co-staining analysis on whole mount first instar larvae with the cell membrane marker α-spectrin and the apical surface marker WGA (19, 22) revealed a strong overlap of extracellular Obst-A and WGA staining in confocal Z-stack sections, orthogonal cross-section projections, and three-dimensional projections (Fig. 3, *D--D″*). Approximately 10 h after hatching larvae undergo apolysis, the separation of epidermal cells from the cuticle occurs, which is followed by the secretion of second instar cuticle (14). In such mid first instar larvae, Obst-A was enriched at the apical cell surface where the assembly zone is expected. Additionally, little Obst-A staining was observed at outer regions of the chitin matrix (Fig. 3, *E–E‴*). It was shown that the loss of *obst-A* caused larval lethality at the transition from first to second instar stage (19). Our findings suggest that Obst-A is present during larval transition in both the outer and therefore first instar cuticle and the newly synthesized second instar cuticle at the cell surface (Fig. 3, *F–F‴*).

We further investigated Obst-A localization by TEM ultrastructure analysis combined with immunogold labeling. In second instar larvae, Obst-A was predominantly localized in the assembly zone at the apical cell surface (Fig. 3*G*). A more detailed study showed that Obst-A staining overlaps with the newly deposited chitin matrix (Fig. 3, *H* and *I*). We did not detect Obst-A labeling in *obst-A* null mutant larvae (Fig. 3*J*). These findings provide evidence that Obst-A is enriched within the assembly zone at the apical epidermal cell surface.

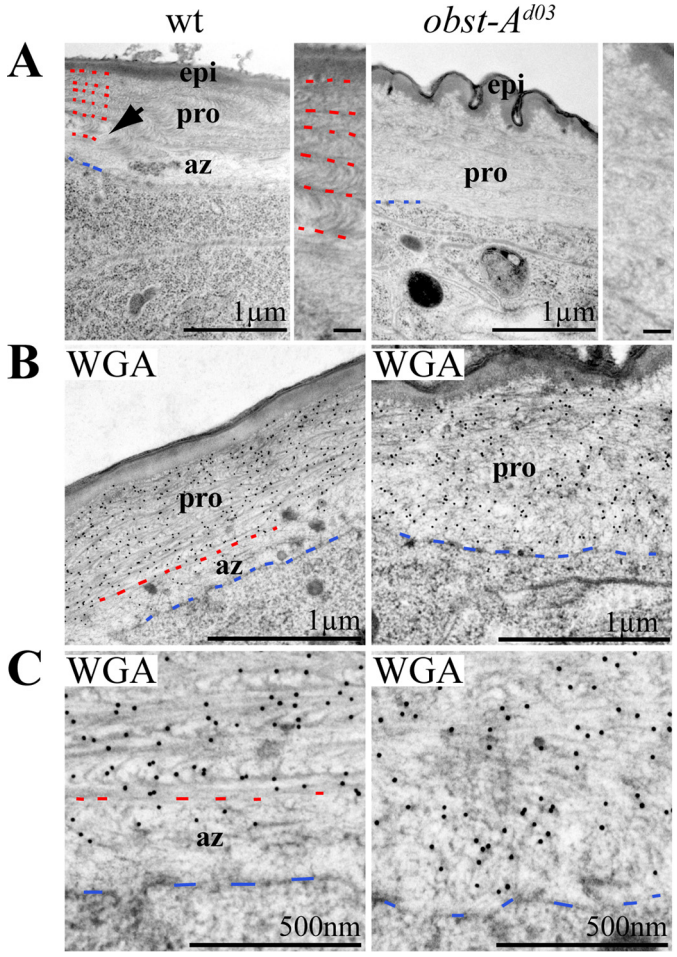

FIGURE 2. **Obst-A organizes chitin matrix structure at the assembly zone.** *A*, the wild type epidermal cuticle (*left panel*) of second instar larvae is stratified into the outermost envelope, the epicuticle, and the prominent inner procuticle. The procuticle contains an increasing number of chitin lamellae. *Arrow* points to the procuticle. *Red dashes* mark borders between chitin layers of the procuticle, and *blue dashes* point to the apical cell membrane. In wild type larvae, the less electron dense assembly zone is localized between apical cell surface and procuticle. In contrast, the assembly zone is largely diminished in *obst-A* mutant larvae ($n = 3$; *right panel*). Rudimentary procuticle organization is detectable within the entire chitin matrix. Magnifications of the procuticle show highly organized chitin matrix in the wild type but impaired architecture in *obst-A* mutants. A wrinkled structure of the epidermal aECM is found in *obst-A* mutants. *Scale bars* in magnifications represent 100 nm. *B* and *C*, overview (*B*) and magnifications (*C*) of the ultrastructure show immunogold-labeled WGA that recognizes chitin. WGA labeling is strongly enriched in the procuticle but less in the assembly zone of wild type second instar larvae. In contrast, in *obst-A* mutant larval epidermis WGA is evenly distributed in the chitin matrix, and a distinct assembly zone is not detected. *Blue dashes* label the apical cell surface, and *red dashes* indicate where the procuticle starts. *Scale bars* represent 1 μm or 500 nm, respectively. *pro*, procuticle; *az*, assembly zone; *epi*, epicuticle.

The assembly zone, as the first aECM layer at the apical cell surface, is located between the epidermal cells and its secretory product, the procuticle (27). At the assembly zone, chitin fibrils arise and are most probably organized into the characteristic lamellae of the arthropod procuticle (14, 29). Because the chitin matrix requires renewal during larval molting, we analyzed essential modulators for chitin maturation and protection. It was shown that newly synthesized chitin is protected by the conserved glycosylphosphatidylinositol-anchored Knk (Knickkopf) protein for organization of the body wall cuticle in *Tribolium* and for cuticle texture in *Drosophila* trachea and epidermis (4, 24, 25). In wild type first instar larvae, Knk was found in the cuticle matrix, showing strong co-localization with chitin. In late *obst-A* mutant first instar larvae, the Knk protein showed normal co-localization with chitin, but Knk levels appeared up-regulated (Fig. 4, *A*–*B*′). Therefore, relative *knk* expression levels were tested in wild type larvae and compared with *obst-A* mutants by qRT-PCR. Approximately 22 h after larval hatching, first instar larvae undergo transition to second instar stage (ecdysis). The first instar stage *knk* levels strongly increased when wild type larvae reached ecdysis and started to molt (Fig. 4*C*). In contrast, in *obst-A* mutants *knk* levels did not increase for ecdysis 22 h after hatching. Instead, *knk* became unusually up-regulated 26 h after hatching (Fig. 4*C*). This late transcript up-regulation is consistent with enriched Knk staining (Fig. 4*B*), suggesting that the dying *obst-A* mutants could try to improve cuticle protection.

Serp and the related Verm (Vermiform) both are conserved deacetylase domain proteins required to improve chitin matrix maturation, stability, and structural durability in embryos (10, 11). Immunofluorescent stainings of first instar wild type larvae showed Serp enrichment at the apical cell surface (Fig. 4, *D* and *D*′). In contrast, the loss of *obst-A* resulted in Serp aggregate-like clusters, which appeared mislocalized within the entire chitin matrix (Fig. 4, *E* and *E*′). Also, Verm was enriched in the first instar stage at the apical cell surface but was mislocalized throughout the whole chitin matrix in *obst-A* mutants (Fig. 4, *G*–*H*′). Additionally, qRT-PCR analysis of the relative expression levels showed declined *serp* and *verm* expression in *obst-A* mutants specifically 22 h after larval hatching, when wild type larvae usually undergo ecdysis (Fig. 4, *F* and *I*). These data indicate that Obst-A is involved in Knk, Serp, and Verm localization and their function at the epidermal cuticle.

Larvae need to establish chitin matrices that withstand mechanical forces. Indeed, pricking of living wild type first instar larvae with a thin glass needle at the posterior lateral epidermis led to small wounds and a little bleeding but was not lethal. Thus, in wild type larvae cuticle, barrier integrity is not severely compromised (19). In contrast, large wounds appeared in pricked *obst-A* mutant first instar larvae, resulting in severe organ spill out, massive loss of hemolymph, and immediate lethality after injury (19). Similar phenotypes of defective cuticle integrity were summarized for UAS-RNAi (interference)-mediated *knk*, *serp*, and *verm* knockdown larvae (Fig. 5*A*), when expressed in the epidermis with the help of the 69BGal4 driver (30, 31). It is of note that the knockdown efficiency of those ranged between 88 and 93% (data not shown) and resulted in larval lethality (Fig. 5*B*). Furthermore, *obst-A* mutant-like cuticle integrity defects were also found in transheterozygous first instar larvae carrying a single mutant allele of *obst-A* and *knk* (*obst-A*/+; *knk*/+), as well as in transheterozygous larvae of *obst-A* and *serp,verm* (*obst-A*/+; *serp,verm*/+) (Fig. 5*A*). These observations further support genetic interaction of *obst-A* with *knk* and with *serp* and *verm* to provide epidermal cuticle integrity.

First instar larvae undergo transition to the second instar stage. Only few hours after larval ecdysis, newly secreted second instar chitin matrix differentiates into the compact procuticle. The process of chitin matrix reorganization is repeated ~48 h

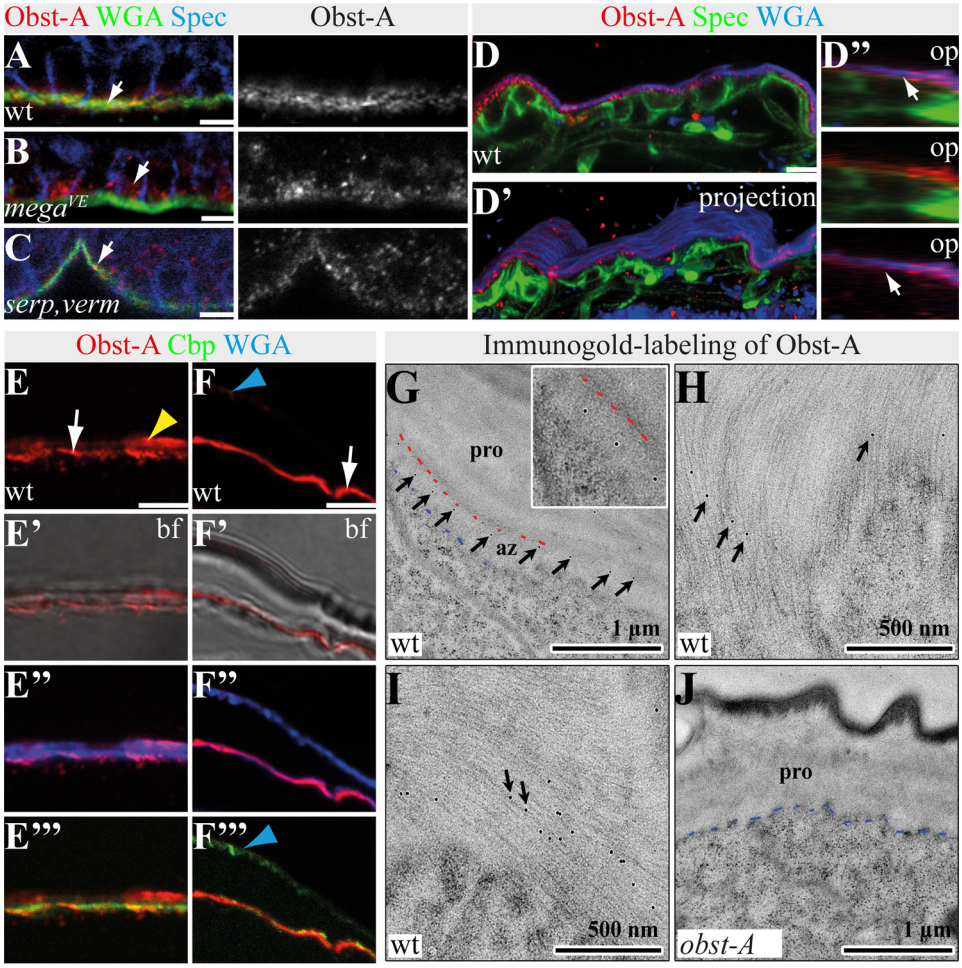

FIGURE 3. **Epidermal Obst-A is localized within the cuticle.** *A–C*, confocal images show epidermal cells of stage 17 embryos labeled with anti-Obst-A (*red*), the membrane marker anti-α-Spectrin (*blue*), and WGA (*green*) marking the apical cell surface (*green*). The single Obst-A channel is presented in *gray*. *Scale bars* indicate 5 μm. *A*, in stage 17 wild type embryos, Obst-A is enriched (*arrow*) at the apical cell surface, which is marked by WGA. Only weak intracellular Obst-A distribution is found within epidermal cells. *Spec* marks plasma membranes of epidermal cells. *B*, in stage 17 *mega* mutant embryos, Obst-A remains in epidermal cells (*arrow*), and extracellular Obst-A staining was reduced. *C*, in stage 17 *serp,verm* mutants, Obst-A was normally enriched at the apical cell surface (*arrow*). *D–D″*, confocal analysis of whole mount staining of a wild type first instar larva labeled with anti-Obst-A (*red*), WGA (*blue*), and anti-α-Spectrin (*green*). Confocal scan (*D*), three-dimensional (*D′*), and orthogonal projections in *D″* of the epidermis demonstrate extracellular Obst-A overlap (*arrows*) with the apical cell surface marker WGA (*D″*, *bottom panel*) but not with α-Spectrin (*D″*, *middle panel*). *E* and *F*, confocal images of larval cross-sections, labeled with Obst-A (*red*), Cbp (chitin, *green*), and WGA (*blue*) and bright field microscopy. *E–F‴*, in mid (*E–E‴*) and late (*F–F‴*) first instar larval epidermis, both newly deposited cuticle and old first instar cuticle are detected (14). Obst-A is localized at the apical cell surface together with newly deposited chitin (*arrows*) and at outer regions (*yellow* and *blue arrowheads*), probably representing the old first instar cuticle. Obst-A staining overlaps with WGA (*E″* and *F″*) and chitin (Cbp, *E‴*, *F‴*). Analysis of first and second instar larvae ($n \geq 20$) is shown. *Scale bars*, 5 μm. *G–J*, immunogold labeling of Obst-A in second instar wild type (*G–I*) and *obst-A* mutant epidermis (*J*). *G*, in second instar wild type larval epidermis, immunogold labeling of Obst-A (*arrows*) is enriched at the apical cell surface but underneath the procuticle. The *inset* shows a high magnification. *Blue dashes* indicate the apical cell surface, and *red dashes* the start of the procuticle. Apical cell surface is at the bottom in all images. *Scale bars* represent 1 μm. *H* and *I*, single or even several immunogold particles labeling Obst-A (*arrows*) overlap with chitin fibrils within the assembly zone. *Scale bars* represent 500 nm. *J*, in *obst-A* null mutant larvae, no immunogold particles were observed at the chitin matrix. *Blue dashes* indicate the apical cell surface. *pro*, procuticle; *az*, assembly zone; *bf*, bright field; *op*, orthogonal projections. *Scale bars*, 1 μm.

after larval hatching for the ecdysis of second into third instar larvae (14). The study of relative expression levels showed strong up-regulation of *obst-A*, *verm*, *serp*, and *knk* during ecdysis into second and third instar. In addition, basic expression levels at intermolt increased from first to third larval stage (Fig. 6, *A–C*). In summary, our studies indicate that Obst-A, Knk, Serp, and Verm could be involved in cuticle assembly and disassembly for larval molting.

After molting, third instar larvae produce almost one chitin matrix lamella per hour. They dramatically increase the number of chitin lamellae up to 50 or even more (14) during a very short time period. A role of Obst-A, Knk, Serp, and Verm was tested in regulating such massive cuticle formation. Relative expression showed strong up-regulation of *obst-A*, *knk*, *serp*, and *verm* at ecdysis from second to third instar. During third instar expression levels of the genes decreased but remained at high levels when compared with earlier larval stages (Fig. 6, *A–C*).

In immunofluorescent studies, WGA was used to detect the apical cell surfaces in *Drosophila* embryos and larvae (19, 21, 23). Similar to those studies, confocal analysis of third instar epidermis revealed WGA accumulation at the apical cell surface and further labeling of the chitin matrix (Fig. 6, *D–I*). Co-labeling experiments showed co-enrichment of Obst-A with WGA at the apical cell surface (Fig. 6*E*). The chitin staining appeared in stratified horizontal lines, probably reflecting the

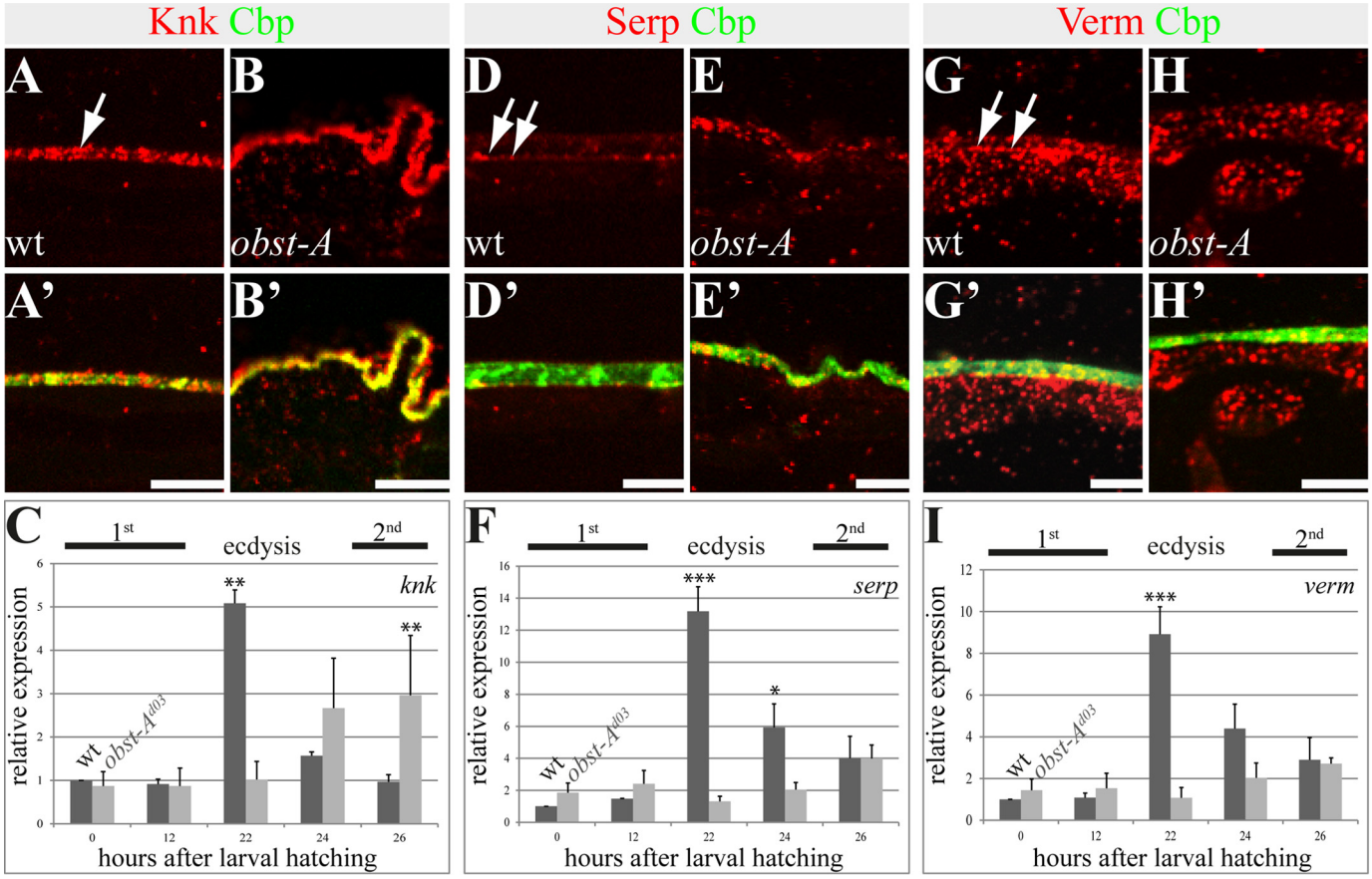

FIGURE 4. **Epidermal localization and expression of the chitin protector Knk and the chitin deacetylases Serp and Verm.** The *top* and *middle panels* show confocal images of first instar larval cross-sections and labeled with anti-Knk (*red*), anti-Serp (*red*), anti-Verm (*red*), and Cbp (chitin, *green*). The *bottom panel* provides qRT-PCR analysis of relative *knk* (*C*), *serp* (*F*), and *verm* (*I*) expression in wild type and *obst-A* null mutant larvae. *A–B′*, Knk localization in wild type (*A* and *A′*) and *obst-A* mutant (*B* and *B′*) epidermis. In late first instar larval epidermis, Knk is distributed in the chitin matrix (*arrow* in *A*) where it co-localizes with the chitin marker Cbp (*A* and *A′*). In late first instar *obst-A* mutant epidermis, Knk staining appeared slightly enriched but revealed a wild type-like distribution (*B* and *B′*). *D–E′*, in wild type mid first instar epidermis, Serp staining is enriched at the apical cell surface (*arrows* in *D*). Serp staining is not distributed throughout the entire chitin matrix, because it only partially overlaps with chitin as detected by Cbp (*D′*). In first instar *obst-A* mutant epidermis, Serp staining is mislocalized and is found throughout the chitin matrix without enrichment at the apical cell surface (*E* and *E′*). *G–H′*, Verm localization in wild type (*G* and *G′*) and *obst-A* mutant (*H* and *H′*) epidermis. Verm staining resembles the Serp pattern. Verm is enriched in the newly deposited chitin matrix (*arrows* in *G*) where it partially overlaps with chitin (*G′*). In first instar *obst-A* mutant epidermis, Verm is mislocalized within the chitin matrix. Analysis of wild type and *obst-A* mutant larvae ($n \geq 20$) is shown. *Scale bars* represent 5 μm. *C*, *F*, and *I*, qRT-PCR analysis of relative expression in wild type and *obst-A* null mutant larvae shows a significant up-regulation of *knk*, *serp*, and *verm* levels 22 h after larval hatching, which corresponds to ecdysis from first to second instar larval stage. In *obst-A* mutants, however, *knk*, *serp*, and *verm* expression is not up-regulated at 22 h after larval hatching. *knk* levels are significantly enriched at 26 h after larval hatching, shortly before *obst-A* mutants start to die. Significance (one-way analysis of variance) is compared with values 0 h after hatching of wild type larvae and indicated by *asterisks*, and standard error of the mean is represented by *bars*. *p* values are represented by asterisks: *, $p < 0.05$; **, $p < 0.01$; and ***, $p < 0.001$.

lamellar procuticle morphology. Confocal Z-stacks and orthogonal projections showed that Obst-A is additionally localized in a dotty pattern along those lamellae-like chitin structures (Fig. 6*F*). In contrast to wild type, in the epidermal cuticle of *serp*, *verm*, and *knk* knockdown third instar larvae, extracellular Obst-A was reduced (Fig. 6, *G–I*). In addition, those knockdown mutants revealed a deformed chitin matrix, although the deformities varied in severity (Fig. 6, *G–I*). Collectively, these findings indicate that Obst-A is enriched at the epidermal apical surface and, in addition, within the outer chitin matrix in third instar larvae. Furthermore, Obst-A localization depends on *serp*, *verm*, and *knk* function.

Analogous to Obst-A, we studied Serp, Verm, and Knk localization in the growing third instar cuticle matrix. Co-labeling studies with WGA detected Serp, Verm, and little Knk enrichment at the apical cell surface. Although Serp and Verm stainings were weak within the stratified chitin matrix (Fig. 7, *A* and *B*), Knk appeared rather distributed toward the chitinous cuticle (Fig. 7*C*). As shown above, *knk* knockdown larvae resulted in a deformed chitin matrix. Consequently, not only Obst-A (Fig. 6*I*), but also Serp and Verm were reduced in the outer chitinous cuticle (Fig. 7, *D* and *E*). Consistent with the well described *Tribolium* Knk cuticle protection function (4), our data provide evidence that also *Drosophila* Knk is strongly required for the newly synthesized chitin matrix within the lamellate procuticle. Moreover, genetic analysis showed severe cuticle defects in transheterozygous *obst-A* and *knk* (*obst-A/+; knk/+*) mutant third instar larvae. Approximately half of the mutant larvae failed to complete molting and possessed the *obst-A* mutant-like wrinkled epidermal cuticle (Fig. 7*F*). In addition, extracellular Serp and Verm stainings were declined, and the chitin matrix was deformed (Fig. 7, *G* and *H*).

Obst-A, Serp, and Verm accumulate at the apical surface, where chitin is modified and packaged into the lamellae. In

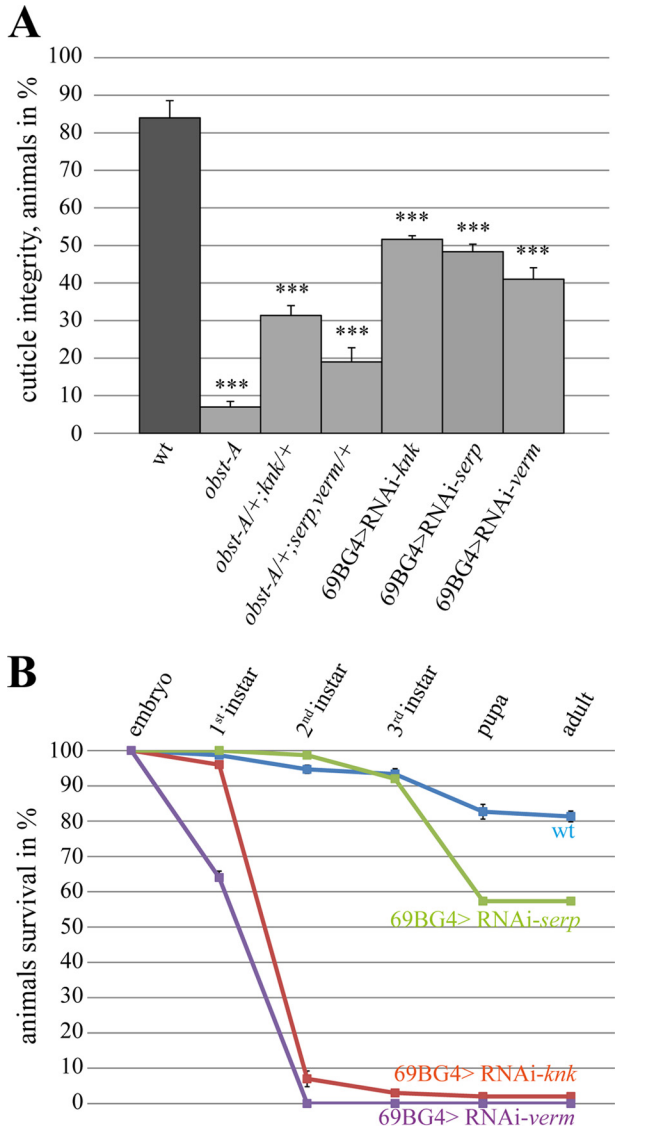

FIGURE 5. ***knk*, *serp*, and *verm* are required for epidermal cuticle integrity and larval survival.** *A*, cuticle integrity test was performed by pricking first instar larvae according to Petkau *et al.* (19). 84% of wild type larvae ($n = 94$) survived pricking without severe wounding, whereas 93% of *obst-A* mutant larvae ($n = 46$) showed severe epidermal disruption, which caused organ spill and immediate lethality. A large number of transheterozygous larvae (*obst-A*/+,*knk*/+ ($n = 60$) and *obst-A*/+,*serp,verm*/+ ($n = 65$)) showed *obst-A* mutant-like cuticle integrity defects. Similar cuticle integrity defects were observed in *knk* (48%, $n = 103$), *serp* (52%, $n = 66$), and *verm* (59%, $n = 58$) knockdown larvae. The *p* values are represented by *asterisks*: *, $p < 0.05$; **, $p < 0.01$; and ***, $p < 0.001$. *B*, survival tests revealed larval lethality for *knk*, *serp*, and *verm* knockdown mutants but not for wild type. The test was repeated four times with $n = 25$ larvae of each genotype. Less than 1% of *verm* knockdown larvae reach the third instar stage. The *error bars* represent the standard error, and *p* values are represented by *asterisks*. Note that the knockdown efficiency for all RNAi lines as determined by qRT-PCR was ~90% (data not shown).

obst-A null mutant first instar larvae, apical enrichment of Serp and Verm was not detectable. Similar phenotypes were observed in transheterozygous *obst-A* and *serp,verm* (*obst-A/+; serp,verm/+*) mutant third instar larvae. Confocal sections and orthogonal projections showed a deformed epidermal chitin matrix and reduced stainings of Knk (Fig. 7, *I–L*). In summary, our data suggest that Obst-A, Serp, and Verm, as well as Knk, genetically interact in packaging and protecting the chitin matrix of the epidermal cuticle.

DISCUSSION

Molting, wounding, and other types of cuticle disruption require complex actions of enzymes and scaffold proteins that form new and remodel existing cuticles throughout development (4, 32, 33). To some extent, chitin synthases and chitinolytic enzymes have been studied in the past (1–7), but little is known about underlying mechanisms that control the assembly, stability, and integrity of newly synthesized cuticles. The assembly zone is the first apical extracellular area where all cuticle components are deposited and the chitin matrix is packaged into the highly ordered procuticle. It has been discussed that the assembly zone is a permeable matrix for components that process into the cuticle (27). Indeed, cuticle proteins and putative enzymes were identified to be part of the assembly zone (27); however, they have not been molecularly characterized.

Our data demonstrate that Obst-A plays a key role in organizing the chitin matrix. Normal chitin levels in *obst-A* null mutants exclude a role in chitin synthesis. Given that Obst-A is required for exoskeletal function at the epidermis (Figs. 1 and 2) (19), we investigated the extracellular region where Obst-A organizes the chitin matrix. Indeed, confocal, ultrastructure, and mutant analyses identify Obst-A as a chitin-binding protein essential for assembly zone formation. Moreover, Obst-A and its partner proteins are required for larval cuticle stability (Fig. 5*A*) (19). In addition, our observations about *obst-A* expression pattern are in line with recent data showing that the loss of *obst-A* results in severe molting defects and lethality shortly after ecdysis to second instar larval stage (19). Collectively, Obst-A is an essential regulator at the apical cell surfaces coordinating chitin matrix formation and thereby promoting epidermal cuticle integrity.

Cuticle defects in *obst-A* mutants could implicate impaired protection of newly synthesized cuticle. In the beetle *Tribolium castaneum*, the Knk protein is required for protection of newly synthesized chitin matrix (4). In the embryonic tracheal matrix, Obst-A maintains extracellular Knk localization, which prevents premature degradation of the cuticle during tracheal tube size control (19). A few hours later at the end of embryogenesis, the dispensable intraluminal chitin matrix becomes cleared by clathrin-mediated endocytosis (21, 22), resulting in a rather thin apical chitin-rich cuticle (23). Here we found that epidermal extracellular Knk co-localization with chitin was not affected in *obst-A* mutants, and conversely weak apical Obst-A enrichment was found in *knk* knockdown larvae. However, *knk* gene and protein levels appeared reduced in the *obst-A* mutants at a time when wild type larvae start to molt. This suggests that chitin matrix protection must be affected. Our findings may not exclude other potential protective proteins (32), and yet uncharacterized *Drosophila* Knk-like proteins (33) could depend on Obst-A. However, the wrinkled cuticle specifically observed in *obst-A* null and transheterozygous *obst-A;knk* mutants and the localization of Obst-A and Knk proteins in the outer cuticle led to the speculative hypothesis that they act in cuticle stability of the newly synthesized and packaged chitin matrix. In summary, our findings might further suggest that

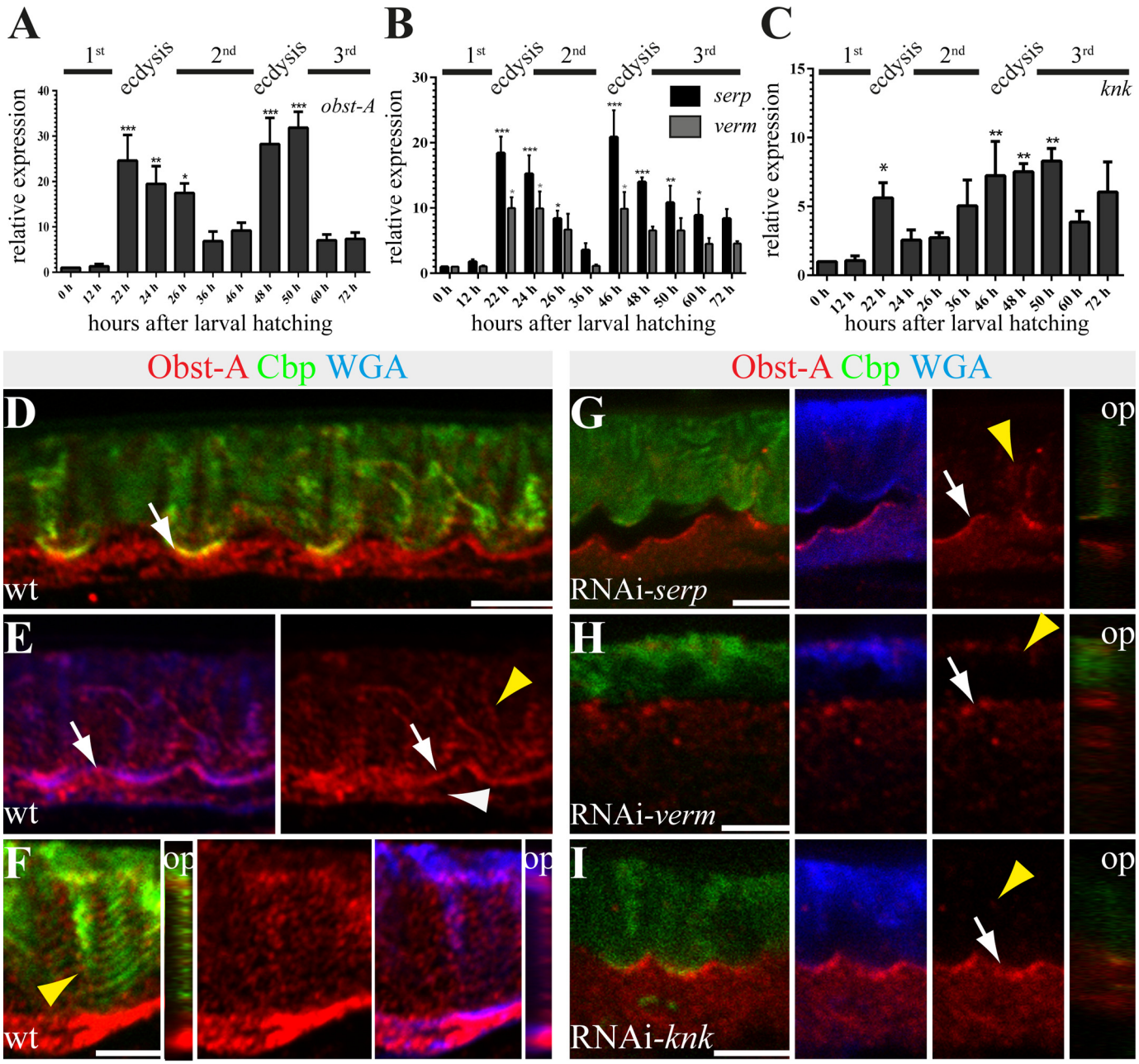

FIGURE 6. **Knk, Serp, and Verm are involved in larval Obst-A expression and its localization within the cuticle.** *A–C*, qRT-PCR analysis shows relative expression levels of *obst-A* (*A*), *serp* and *verm* (*B*), and *knk* (*C*) throughout larval development. *obst-A*, *serp*, *verm*, and *knk* expression levels are up-regulated during ecdysis to second and third instar stages. Significance (one-way analysis of variance) is compared with values 0 h after larval hatching and indicated by *asterisks*, and S.E. is represented by *bars*. *p* values are represented by *asterisks*: *, $p < 0.05$; **, $p < 0.01$; and ***, $p < 0.001$. *D–I*, confocal images of third instar larval cross-sections, labeled with Obst-A (*red*), Cbp (chitin, *green*), and WGA (*blue*). Orthogonal projections of Z-stacks are depicted in small images. *D* and *E*, in wild type third instar larvae, chitin (Cbp, *green*) and the apical cell surface marker WGA (*blue*) co-localize with Obst-A (*red*) staining at the epidermal apical cell surface (*white arrows*). Obst-A (*red*) alone is depicted at the *right side*. Obst-A is enriched at the apical cell surface, and in addition lower levels were detected intracellularly (*white arrowhead*) and in the chitin-rich procuticle (*yellow arrowhead*). *F*, the third instar procuticle consists of several distinct chitin lamellae, as indicated by the stratified chitin staining. Obst-A co-localizes with the lamella-like chitin (*arrowhead*, *left image*) and with WGA (*blue*) detected in the chitin matrix. Orthogonal projections are presented in small images, and Obst-A is alone in the central image. *G–I*, *serp*, *verm*, and *knk* knockdown larvae ($n \geq 18$) show defective chitin matrix organization and extracellular Obst-A staining appeared reduced (*yellow arrowheads*), but Obst-A enrichment at the apical cell surface is detected in *serp* and *knk* and partially in *verm* knockdown (*arrows*). The cuticle is detached in *serp*, but not in *knk* or *verm* knockdown larvae. *op*, orthogonal projections. *Scale bars* represent 5 μm.

aspects of *obst-A* mutant cuticle phenotypes could be the result of mistimed or ectopic degradation of chitin in the exoskeleton.

The procuticle is capable of extending throughout larval development, whereas its integrity remains stable. Previous data about Obst-A binding with chitin and our ultrastructure observations suggest that Obst-A could play a role in coordinating chitin scaffold formation. This would be consistent with gene expression data, protein localization, and genetic studies that propose a genetic link of *obst-A* with *serp* and *verm* in organizing maturation of the epidermal cuticle throughout larval development. Our data further suggest that Obst-A proteins may recruit chitin fibrils at the apical cell surface to organize

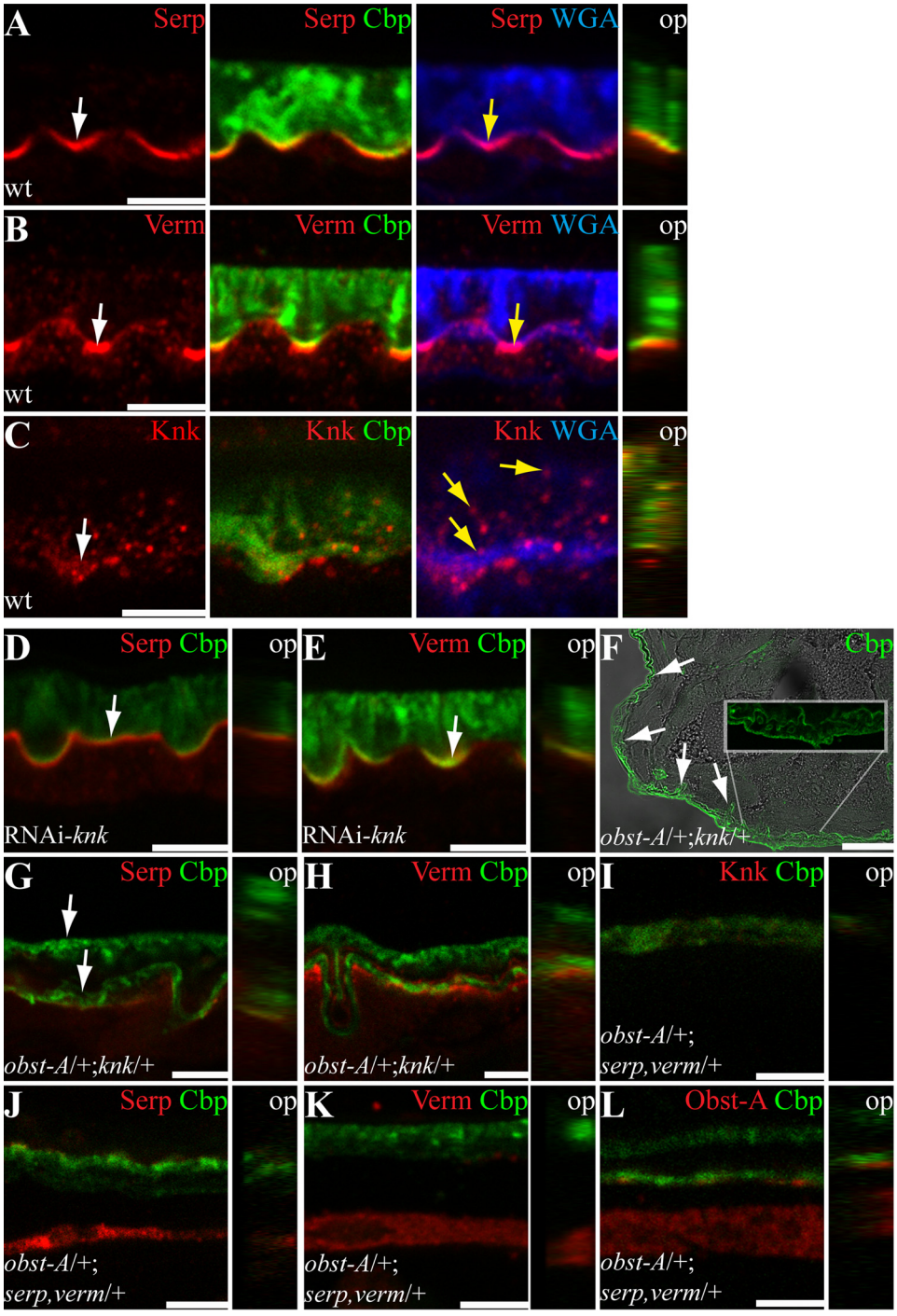

FIGURE 7. **Genetic control of epidermal cuticle organization in *Drosophila* larvae.** Confocal images of third instar larval cross-sections, labeled with Serp (*red* in *A*, *D*, and *G*), Verm (*red* in *B*, *E*, and *H*), Knk (*red*; *C* and *I*), and Obst-A (*red*; *F*). Chitin is detected by Cbp (*green*) and the apical cell surface by WGA (*blue*). Orthogonal projections of Z-stacks are depicted in small images. *A* and *B*, Serp and Verm are strongly enriched at the apical cell surface (*white arrows*) overlapping with chitin (Cbp, *green*) and WGA (*yellow arrows*). Orthogonal projections confirm enrichment at the apical cell surface overlapping with the chitin matrix. *C*, Knk signal is enriched (*white arrow*) but not restricted to the apical cell surface. Knk is distributed throughout the whole chitinous procuticle (*yellow arrows*). The orthogonal projection visualizes the distribution of Knk within the whole procuticle. *D* and *E*, the RNAi-mediated knockdown of *knk* shows reduced extracellular Serp (*D*) and Verm (*E*) staining, which, however, appeared still enriched at the apical cell surface (*arrows*). *F–H*, in transheterozygous *obst-A*/+; *knk*/+ third instar larvae ($n = 6$), chitin matrix is deformed, cuticle molting is defective (*arrows* in *F* and *G*), and extracellular Serp (*G*) and Verm (*H*) stainings are decreased. Approximately 50% of such mutant larvae frequently show *obst-A* mutant-like wrinkled epidermal cuticle (*arrows* in *F*) but not detached cuticle. The *inset* highlights the wrinkled newly synthesized cuticle and the outer old cuticle. *I–L*, in transheterozygous *obst-A*/+;*serp,verm*/+ third instar larvae ($n = 14$), chitin matrix organization is defective, and the cuticle is frequently detached from the epidermis. These mutants show reduced extracellular Knk (*red*; *I*), Serp (*red*; *J*), Verm (*red*; *K*), and Obst-A (*red*; *L*) stainings. Transheterozygous mutants show strong reduction or loss of Obst-A, Serp, and Verm accumulation at the apical cell surface. The transheterozygous *obst-A*/+;*serp,verm*/+ mutants show detached (6 of 14) but not wrinkled cuticle. *op*, orthogonal projections. *Scale bars* represent 5 and 50 μm in *F*, respectively.

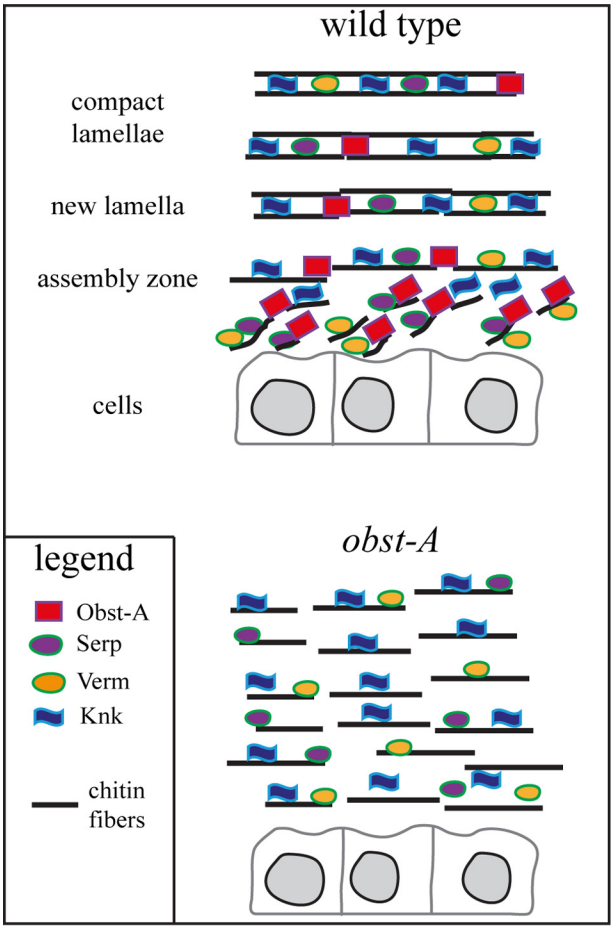

FIGURE 8. **Obst-A organizes the aECM at the apical cell surface.** Schematic model illustrates Obst-A in the cuticle. Our data provide evidence that Obst-A arranges chitin matrix maturation and protection at the apical cell surface. We propose that Obst-A controls chitin scaffold formation. Obst-A acts in a common pathway with the deacetylation enzymes Serp and Verm and with the chitin protector Knk to mature, stabilize, and protect the aECM within the cuticle.

their packaging and maturation into a more compact procuticle. In addition, we observed Obst-A scattering along the stratified chitin lamellae in third instar larval cuticle. Therefore, it is also possible that Obst-A is involved in providing stability of the outer epidermal cuticle.

Previously, it was described that the zona pellucida protein Piopio provides a structural network in trachea (34) that may link the apical epithelial cell surface with the overlaying aECM at the epidermis (28). In addition, Alas (δ-aminolevulinate synthase), expressed in the hepatocyte-like oenocytes, is involved in formation of a dityrosine network at the apical cell surface to resist hydrostatic pressure of the hemolymph and to prevent dehydration (35). Local detachment between cell surface and cuticle observed in *piopio* and *alas* mutants (28, 35) was also identified in *obst-A* null mutants (Fig. 1*B*). Interestingly, cuticle detachment was found in *obst-A* mutants, *serp* knockdown larvae and in the transheterozygous *obst-A serp,verm* mutants. Because of defective cuticle structure in *obst-A* mutants, we speculate that cuticle formation at the apical cell surface, likely within the assembly zone, affects essential aspects of cell adhesion to the aECM (28).

Our data provide evidence that Obst-A is required for the assembly zone formation. Whether Obst-A may act in the elongation or ordering of chitin filaments or whether it prevents premature chitin fibril assembly remains elusive. However, our data propose that Obst-A provides a well structured chitin scaffold for deacetylation enzymes to mature and improve aECM stability and integrity. Furthermore, genetic studies suggest that Obst-A is linked to Knk-mediated protection of the newly synthesized cuticle (Fig. 8). All insects establish compact and structured exoskeletal cuticles at their outermost body parts (4, 29, 32, 33, 36, 37). Our data argue that structural similarities of the body wall cuticle and molecular conservation of involved proteins (8, 9, 15–19, 38–40) point toward a highly conserved mechanism of procuticle formation among chitinous invertebrates.

Acknowledgments—We are very grateful to Anne Uv, Peter J. Bryant, Richard G. Fehon, Stefan Luschnig, Bernard Moussian, Reinhard Schuh, and Markus Affolter for sharing flies and reagents. We thank Melanie Homberg, Yasmine Port, Reinhard Schuh, André Völzmann, Nadine Weinstock, and Anna-Lena Wulf for comments on the manuscript. We appreciate experimental assistance by Melanie Thielisch, Kapil R. Patil, Georg Petkau, and Michael Beilharz. Very special thanks go to Michael Hoch in Bonn and Thomas Magin in Leipzig for great support.

REFERENCES

1. Kramer, K. J., and Muthukrishnan, S. (2005) Chitin metabolism in insects. In *Comprehensive Molecular Insect Science* (Gilbert, L. I., Iatrou, K., and Gill, S. S., eds) pp. 11–144, Elsevier Science Publishers B.V., Amsterdam
2. Merzendorfer, H., and Zimoch, L. (2003) Chitin metabolism in insects: structure, function and regulation of chitin synthases and chitinases. *J. Exp. Biol.* **206,** 4393–4412
3. Merzendorfer, H. (2006) Insect chitin synthases: a review. *J. Comp. Physiol. B* **176,** 1–15
4. Chaudhari, S. S., Arakane, Y., Specht, C. A., Moussian, B., Boyle, D. L., Park, Y., Kramer, K. J., Beeman, R. W., and Muthukrishnan S (2011) Knickkopf protein protects and organizes chitin in the newly synthesized insect exoskeleton. *Proc. Natl. Acad. Sci. U.S.A.* **108,** 17028–17033
5. Arakane, Y., and Muthukrishnan, S. (2010) Insect chitinase and chitinase-like proteins. *Cell Mol. Life Sci.* **67,** 201–216
6. Zhu, Q., Arakane, Y., Banerjee, D., Beeman, R. W., Kramer, K. J., and Muthukrishnan, S. (2008) Domain organization and phylogenetic analysis of the chitinase-like family of proteins in three species of insects. *Insect Biochem. Mol. Biol.* **38,** 452–466
7. Moussian, B. (2010) Recent advantages in understanding mechanisms of insect cuticle differentiation. *Insect Biochem. Mol. Biol.* **40,** 363–375
8. Arakane, Y., Dixit, R., Begum, K., Park, Y., Specht, C. A., Merzendorfer, H., Kramer, K. J., Muthukrishnan, S., and Beeman, R. W. (2009) Analysis of functions of the chitin deacetylase gene family in *Tribolium castaneum*. *Insect Biochem. Mol. Biol.* **39,** 355–365
9. Dixit, R., Arakane, Y., Specht, C. A., Richard, C., Kramer, K. J., Beeman, R. W., and Muthukrishnan, S. (2008) Domain organization and phylogenetic analysis of proteins from the chitin deacetylase gene family of *Tribolium castaneum* and three other species of insects. *Insect Biochem. Mol. Biol.* **38,** 440–451
10. Luschnig, S., Bätz, T., Armbruster, K., and Krasnow, M. A. (2006) Serpentine and vermiform encode matrix proteins with chitin binding and deacetylation domains that limit tracheal tube length in *Drosophila*. *Curr. Biol.* **16,** 186–194
11. Wang, S., Jayaram, S. A., Hemphälä, J., Senti, K. A., Tsarouhas, V., Jin, H., and Samakovlis, C. (2006) Septate-junction-dependent luminal deposition of chitin deacetylases restricts tube elongation in the *Drosophila* tra-

chea. *Curr. Biol.* **16,** 180–185
12. Hsiao, Y. C., Chen, C. N., Chen, Y. T., and Yang, T. L. (2013) Controlling branching structure formation of the salivary gland by the degree of chitosan deacetylation. *Acta Biomater.* **9,** 8214–8223
13. Yang, T. L. (2011) Chitin-based materials in tissue engineering: applications in soft tissue and epithelial organ. *Int. J. Mol. Sci.* **12,** 1936–1963
14. Kaznowski, C. E., Schneiderman, H. A., and Bryant, P. J. (1985) Cuticle secretion during larval growth in *Drosophila melanogaster*. *J. Insect Physiol.* **31,** 801–813
15. Behr, M., and Hoch, M. (2005) Identification of the novel evolutionary conserved obstructor multigene family in invertebrates. *FEBS Lett.* **579,** 6827–6833
16. Jasrapuria, S., Arakane, Y., Osman, G., Kramer, K. J., Beeman, R. W., and Muthukrishnan, S. (2010) Genes encoding proteins with peritrophin A-type chitin-binding domains in *Tribolium castaneum* are grouped into three distinct families based on phylogeny, expression and function. *Insect Biochem. Mol. Biol.* **40,** 214–227
17. Jasrapuria, S., Specht, C. A., Kramer, K. J., Beeman, R. W., and Muthukrishnan, S. (2012) Gene families of cuticular proteins analogous to peritrophins (CPAPs) in *Tribolium castaneum* have diverse functions. *PLoS One* **7,** e49844
18. Willis, J. H. (2010) Structural cuticular proteins from arthropods: annotation, nomenclature, and sequence characteristics in the genomics era. *Insect Biochem. Mol. Biol.* **40,** 189–204
19. Petkau, G., Wingen, C., Jussen, L. C., Radtke, T., and Behr, M. (2012) Obstructor-A is required for epithelial extracellular matrix dynamics, exoskeleton function, and tubulogenesis. *J. Biol. Chem.* **287,** 21396–21405
20. Behr, M., Riedel, D., and Schuh, R. (2003) The claudin-like Megatrachea is essential in septate junctions for the epithelial barrier function in *Drosophila*. *Dev. Cell* **5,** 611–620
21. Stümpges, B., and Behr, M. (2011) Time-specific regulation of airway clearance by the *Drosophila* J-domain transmembrane protein Wurst. *FEBS Lett.* **585,** 3316–3321
22. Behr, M., Wingen, C., Wolf, C., Schuh, R., and Hoch, M. (2007) Wurst is essential for airway clearance and respiratory-tube size control. *Nat. Cell Biol.* **9,** 847–853
23. Tonning, A., Hemphälä, J., Tång, E., Nannmark, U., Samakovlis, C., and Uv, A. (2005) A transient luminal chitinous matrix is required to model epithelial tube diameter in the *Drosophila* trachea. *Dev. Cell* **9,** 423–430
24. Moussian, B., Tång, E., Tonning, A., Helms, S., Schwarz, H., Nüsslein-Volhard, C., and Uv, A. E. (2006) *Drosophila* Knickkopf and Retroactive are needed for epithelial tube growth and cuticle differentiation through their specific requirement for chitin filament organization. *Development* **133,** 163–171
25. Moussian, B., Veerkamp, J., Müller, U., and Schwarz, H. (2007) Assembly of the *Drosophila* larval exoskeleton requires controlled secretion and shaping of the apical plasma membrane. *Matrix Biol.* **26,** 337–347
26. Peters, W., and Latka, I. (1986) Electron microscopic localization of chitin using colloidal gold labelled with wheat germ agglutinin. *Histochemistry* **84,** 155–160
27. Wolfgang, W. J., Fristrom, D., and Fristrom, J. W. (1987) An assembly zone antigen of the insect cuticle. *Tissue Cell* **19,** 827–838
28. Bökel, C., Prokop, A., and Brown, N. H. (2005) Papillotte and Piopio: *Drosophila* ZP-domain proteins are required for cell adhesion to the apical extracellular matrix and microtubule organization. *J. Cell Sci.* **118,** 633–642
29. Wolfgang, W. J., and Riddiford, L. M. (1986) Larval cuticular morphogenesis in the tobacco hornworm, *Manduca sexta*, and its hormonal regulation. *Dev. Biol.* **113,** 305–316
30. Brand, A. H., and Perrimon, N. (1993) Targeted gene expression as a means of altering cell fates and generating dominant phenotypes. *Development* **118,** 401–415
31. Dietzl, G., Chen, D., Schnorrer, F., Su, K. C., Barinova, Y., Fellner, M., Gasser, B., Kinsey, K., Oppel, S., Scheiblauer, S., Couto, A., Marra, V., Keleman, K., and Dickson, B. J. (2007) A genome-wide transgenic RNAi library for conditional gene inactivation in *Drosophila*. *Nature* **448,** 151–156
32. Chaudhari, S. S., Arakane, Y., Specht, C. A., Moussian, B., Kramer, K. J., Muthukrishnan, S., and Beeman, R. W. (2013) Retroactive maintains cuticle integrity by promoting the trafficking of Knickkopf into the procuticle of *Tribolium castaneum*. *PLoS Genet.* **9,** e1003268
33. Chaudhari, S. S., Moussian, B., Specht, C. A., Arakane, Y., Kramer, K. J., Beeman, R. W., and Muthukrishnan, S. (2014) Functional specialization among members of knickkopf family of proteins in insect cuticle organization. *PLoS Genet.* **10,** e1004537
34. Jaźwińska, A., Ribeiro, C., and Affolter, M. (2003) Epithelial tube morphogenesis during *Drosophila* tracheal development requires Piopio, a luminal ZP protein. *Nat. Cell Biol.* **5,** 895–901
35. Shaik, K. S., Meyer, F., Vázquez, A. V., Flötenmeyer, M., Cerdán, M. E., and Moussian, B. (2012) δ-Aminolevulinate synthase is required for apical transcellular barrier formation in the skin of the *Drosophila* larva. *Eur. J. Cell Biol.* **91,** 204–215
36. Arakane, Y., Lomakin, J., Gehrke, S. H., Hiromasa, Y., Tomich, J. M., Muthukrishnan, S., Beeman, R. W., Kramer, K. J., and Kanost, M. R. (2012) Formation of rigid, non-flight forewings (elytra) of a beetle requires two major cuticular proteins. *PLoS Genet.* **8,** e1002682
37. Noh, M. Y., Kramer, K. J., Muthukrishnan, S., Kanost, M. R., Beeman, R. W., and Arakane, Y. (2014) Two major cuticular proteins are required for assembly of horizontal laminae and vertical pore canals in rigid cuticle of *Tribolium castaneum*. *Insect Biochem. Mol. Biol.* **53,** 22–29
38. Nisole, A., Stewart, D., Bowman, S., Zhang, D., Krell, P. J., Doucet, D., and Cusson, M. (2010) Cloning and characterization of a Gasp homolog from the spruce budworm, Choristoneura fumiferana, and its putative role in cuticle formation. *J. Insect Physiol.* **56,** 1427–1435
39. Tiklová, K., Tsarouhas, V., and Samakovlis, C. (2013) Control of airway tube diameter and integrity by secreted chitin-binding proteins in *Drosophila*. *PLoS One* **8,** e67415
40. Barry, M. K., Triplett, A. A., and Christensen, A. C. (1999) A peritrophin-like protein expressed in the embryonic tracheae of *Drosophila melanogaster*. *Insect Biochem. Mol. Biol.* **129,** 319–327